RESEARCH PAPER

Optimization of Stereotactic Body Radiation Therapy for Liver Metastases: A Comparative Study of Coplanar and Non-Coplanar VMAT Techniques

Rajhans Kumar[1*], Santosh Kumar [2], Satya Kumar[2], Y.P.Singh [1]

[1]Institute of applied science, Mangalayatan University, Beswan, Aligarh -202146
[2]State Cancer Institute IGIMS, Patna – 800014

***Correspondence author:** Rajhans Kumar
*Institute of applied science, Mangalayatan University, Beswan, Aligarh -202146.

Abstract

Background: This study aims to evaluate whether non-coplanar VMAT beam arrangements provide dosimetric advantages over coplanar configurations in stereotactic body radiotherapy (SBRT) for liver metastases.

Methods: We conducted a retrospective review of eleven patients who had received SBRT for liver metastases in our department. Two VMAT SBRT plans were generated per patient using the Monaco version 6.01 TPS, configured for an Elekta Versa HD machine with 6-MV FFF beams. The non-coplanar VMAT (NC-VMAT) plans consisted of three half arcs with couch angles of 15°, 30°, and 350°, using arc spans of 0°–180° counter-clockwise and 180°–179° clockwise. Coplanar VMAT (C-VMAT) plans generated with a half arc. All plan prescribed to 42 Gy in 6 fractions. Dosimetric and technical parameters were collected and statistically compared to assess performance differences between the two planning techniques..

Results: Target coverage metrics, including V100, V95, conformity index (CI), Homogeneity index(HI) and gradient index (GD), were comparable between NC-VMAT and C-VMAT plans. NC-VMAT achieved slightly improved dose homogeneity (HI: 1.17 vs. 1.20) and reduced integral dose. Mean liver dose was lower with NC-VMAT (10.12 ± 2.18 Gy) compared with C-VMAT (11.2 ± 1.84 Gy). Most OAR doses were within RTOG limits for both techniques, with NC-VMAT showing reduced maximum doses to the spinal cord, stomach, heart, and ribs. Overall monitor units were slightly lower for NC-VMAT (2096.6 ± 686.8) than C-VMAT (2239.3 ± 522.6).

Conclusion: Non-coplanar VMAT demonstrated modest dosimetric advantages over coplanar VMAT for liver SBRT, including improved dose homogeneity, reduced mean liver dose, lower integral dose, and reduced exposure to several critical organs. Target coverage remained comparable between techniques. These findings suggest that incorporating non-coplanar arcs may provide clinically meaningful dosimetric benefits in liver SBRT planning.

Keywords: SBRT,liver metastases, non-coplanar VMAT, coplanar VMAT, dosimetric parameters

How to cite this article: Kumar R, Kumar S, Kumar S, Singh YP. Optimization of Stereotactic Body Radiation Therapy for Liver Metastases: A Comparative Study of Coplanar and Non-Coplanar VMAT Techniques. Int J Drug Deliv Technol. 2026;16(32s):569-577. DOI: 10.25258/ijddt.16.32s.66.

Introduction:

Liver metastases often develop from primary cancers, most commonly colorectal and breast carcinoma [1]. In patients with oligometastatic disease, the liver may be the only site of metastasis, as defined by recent ESTRO–EORTC consensus guidelines [2]. Surgical resection can improve survival, particularly in colorectal cancer, but nearly 80% of patients are not suitable due to medical comorbidities or tumor location [3].

For that ineligible for surgery, local therapies such as radiofrequency ablation, microwave ablation, cryoablation, or transarterial embolization may be considered [4]. These techniques, however, have limitations, including invasiveness and reduced effectiveness for tumors more than 3 cm or near critical structures such as major vessels, bile ducts, or the diaphragm [5].

SBRT also called stereotactic ablative radiotherapy (SABR), has emerged as a noninvasive alternative for both primary and metastatic liver tumors [6]. In SBRT, high-dose treatment is delivered in a small set of fractions with a rapid reduction in dose beyond the target volume, allowing precise tumor targeting while sparing surrounding healthy tissues. Studies have shown that SBRT can achieve excellent local control and improve survival in selected patients. Its use has increased due to its ability to minimize exposure to normal liver tissue and reduce the risk of radiation-induced liver disease [7-9].

Colorectal cancer remains the most frequent source of liver metastases, followed by breast, gastrointestinal, lung, melanoma, and bladder cancers [10]. Only 10%–20% of patients are eligible for surgical resection; the remainder are managed with systemic therapy or noninvasive local treatments such as SBRT [11,12]. Enhancement of imaging modalities, motion management, and treatment planning have further improved the precision and safety of SBRT [13]. Treatment planning typically follows Radiation Therapy Oncology Group (RTOG) guidelines, which provide dose constraints for organs at risk and criteria for target coverage, ensuring consistent treatment quality and reduced toxicity [14,15].

Modern SBRT techniques benefit from image-guided technologies for accurate tumor visualization before

*Author for Correspondence: Rajhans Kumar

and during treatment [16]. Motion management strategies, such as breath-holding, further enhance delivery precision. VMAT offers high dose conformity with shorter treatment times compared to IMRT and 3D-CRT, making it an effective approach for SBRT [17-19]. The use of VMAT with FFF photon beams has become common. Additionally, non-coplanar beam arrangements have been shown to improve dose conformity and further limit radiation exposure to surrounding healthy tissues [20,21].

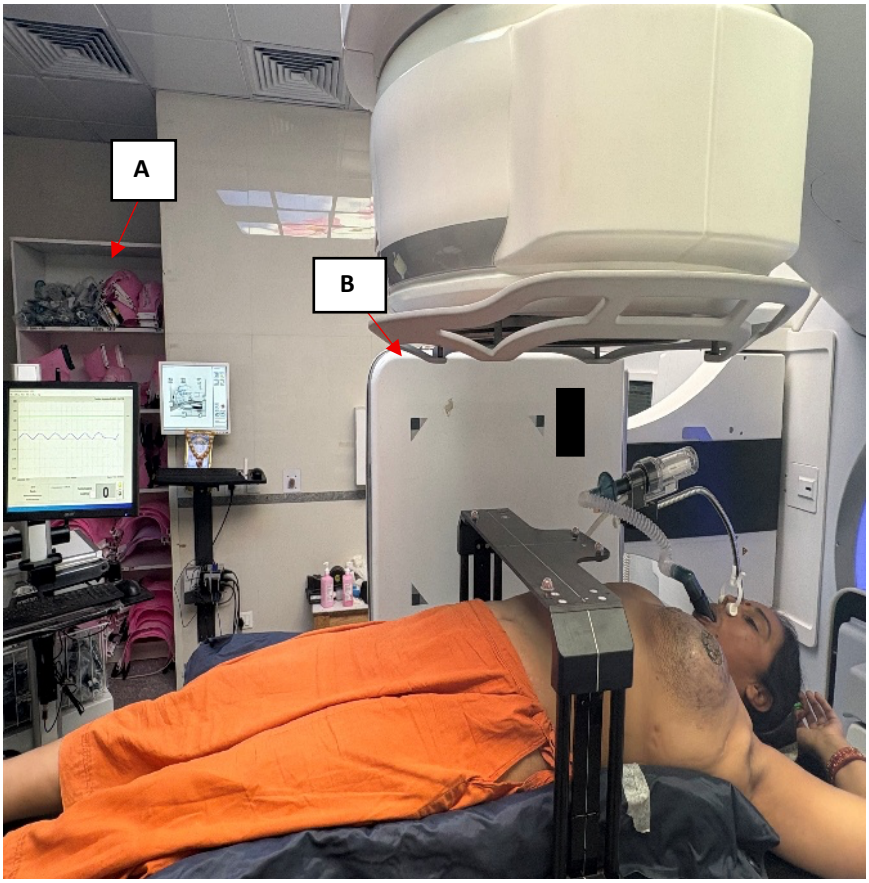

Figure 1. Integrated setup for high-precision radiotherapy: (A) the Active Breathing Coordinator (ABC), which is used to control respiratory motion of the PTV, and (B) the Hexapod couch system, which provides precise patient alignment through six-degree-of-freedom corrections.

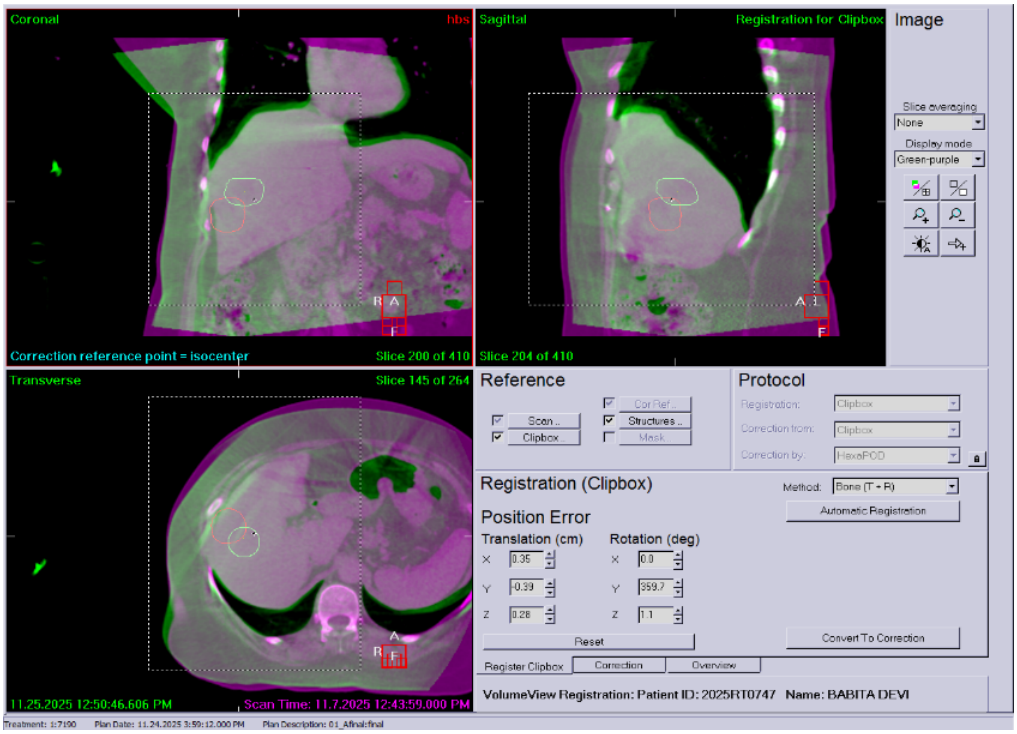

Figure 2. CBCT-Based Patient Positioning Followed by Six-Degree-of-Freedom Hexapod Couch Adjustment in the Same Treatment Session

Materials and Methods:

A total of eleven SBRT-treated liver metastasis patients were examined retrospectively at our institution between June 2022 and October 2025. The group consisted of 8 women and 3 men, aged 41–63 years (mean ± SD: 50.6 ± 8.01 years). Primary tumor sites were breast (n=4), colorectal (n=3), periampullary (n=2), gallbladder (n=1), and cervix (n=1), involving 28 metastatic liver sites. Treatment consisted of 42 Gy delivered in six fractions for every patient.

No of patients	11
Gender	8 Women 3 Men
Age	41-63 (Mean50.6±8.01) Years
Primary site	4-breast,3-colorectal,,2-Periampullary,1-Gallbladder,1 cervix
No. of lession	28
Prescribed dose	42 Gy in 6 fractions

Table 1. Profile Summary of the Chosen Patients.

Immobilization and image acquisition

CT simulation was performed using an Optima GE Healthcare 16-slice scanner from the nipple to the pelvis with a slice thickness of 1 mm. Patients positioned supine with a neutral neck posture and arms raised above the head, and immobilized using a Vac-Lok or cast system to ensure reproducible setup. Because the liver moves during respiration, motion management is essential. Active Breath Control (ABC, Elekta) was used to manage motion in this study. Patients were trained by a technician to perform breath-hold exercises and instructed to practice at home, inhaling 1.2 liters of oxygen and holding their breath for 20 seconds during each simulation.

MRI /PET (Positron Emission Tomography) scans provide useful anatomical information, they are generally not fused with the planning CT because it is usually acquired during free breathing, whereas the planning CT uses the ABC technique for motion control. Nevertheless, MRI images can be referenced to guide accurate target volume delineation. The lesions identified on the portal venous phase of the CT scan were delineated as the gross tumor volume (GTV). In SBRT, there is generally no need to define a separate clinical target volume (CTV). For PTV generation in this study, a 7 mm margin was added in both radial and craniocaudal directions of GTV, taking advantage of daily image-guided radiotherapy and the use of the ABC technique to account for residual movement and setup uncertainties. OARs contoured Liver , Heart, Kidneys, Stomach , Duodenum ,Bowel bag, PORV Spine, R 0ibs , chestwall using .RTOG Guidelines 1112[21].

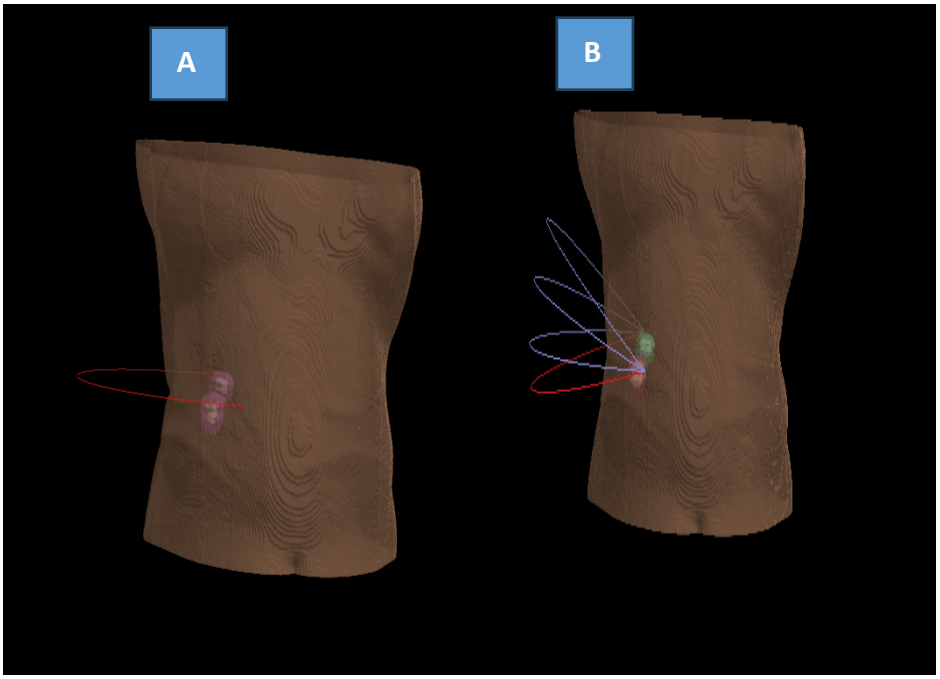

Figure 3.3-D Beam configuration for coplanar and non-coplanar VMAT planning. (A) Coplanar VMAT plan illustrating the use of half-arc. (B) Non-coplanar VMAT (NC-VMAT) arrangement consisting of two counter-clockwise (CCW) half-arcs from 0° to 180° with couch rotations of 15° and 30°, one clockwise (CW) gantry arc from 180° to 179° with a couch rotation of 350°, and an additional half coplanar arc.

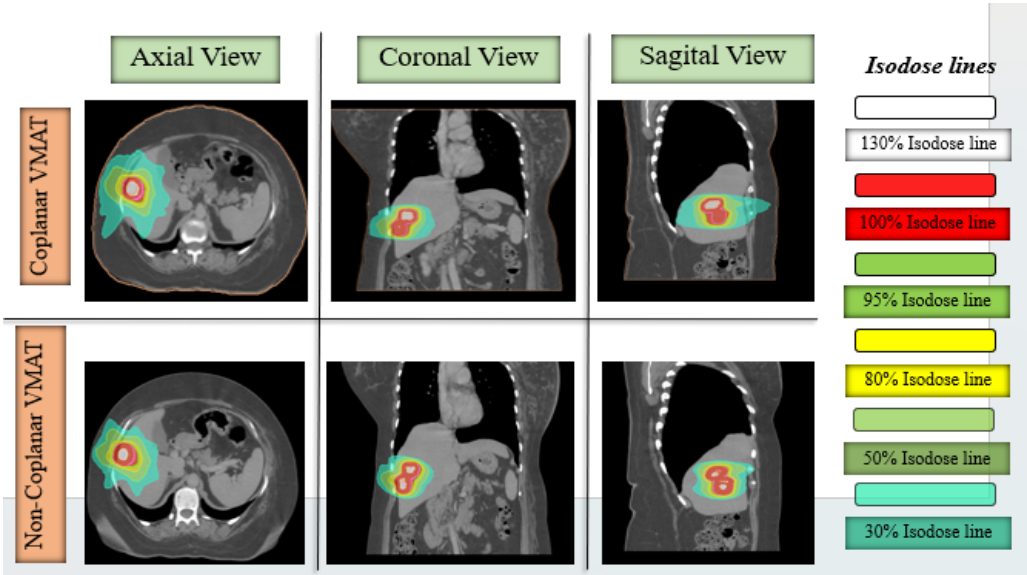

Figure 4: Co-planar and Non-coplanr view

Treatment Planning:

Two SBRT VMAT plans (C and NC) were generated for every patient using 6-MV FFF photons on the Elekta Versa HD system with an Agility collimator. C-VMAT plans consisted of four half-arcs in a counter-clockwise (CCW) direction from 0° to 180°. NC-VMAT plans included two half-arcs in the CCW direction (0°–180°) with couch rotations of 15° ,30°, one clockwise (CW) gantry arc from 180°–179° with a couch rotation of 350° and additional a half coplanar arc used.

A single medical physicist prepared all plans in the Monaco treatment planning system (version 6.00.01). A 0.3 cm grid spacing was used and dose calculations performed with the Monte Carlo algorithm, maintaining a maximum statistical uncertainty of 1%. The minimum segment width was set at 0.5 cm, fluence smoothing was applied at a medium level, and a maximum of 150 control points per arc was used. The treatment plan aimed for a minimum of 95% of the PTV to be covered by the 100% of prescribed dose. It was also required that at least 95% of the prescription dose received more than 98% of the intended dose. A localized hotspot of up to 130% of the prescribed dose was allowed within the GTV to accommodate acceptable dose variation. The dose constraints applied

to the Liver–PTV (700 cc) included a mean dose of 15.2 Gy. The PRV spinal cord limit was set at a D0.05cc of 25 Gy. The bilateral kidneys were restricted to a mean dose of 10 Gy. For the chest wall, the V30 was limited to 30 cc. Dose limits for the bowel and stomach were set at D0.05cc < 30 Gy. The heart constraint was D0.05cc < 12 Gy, and the ribs were limited to a D2ml < 27 Gy. All planning objectives for the PTV and organ-at-risk (OAR) dose constraints were based on the RTOG 1112 guidelines.

Plan Evaluation:

Monitor units were captured for each treatment plan, and comparative evaluation was performed using DVH parameters, focusing on PTV coverage and OAR dose distributions). The parameters used to evaluate PTV coverage were V100% and V95%. In addition, the volumes receiving 110% (V110%), 100% (V100%), and 50% (V50%) of the prescribed dose, along with the total PTV volume, were considered for calculating the CI, HI, and GI as described below.

CI =VPI /PTV Volume [22]

Where VPI is Volume receiving prescription isodose.

HI =(D2-D98)/D50 [23]

D2, D98, D98 dose received by 2%,98% and 50% of the PTV respectively.

GI = 50% Prescription Isodose Volume/ Prescription isodose volume [24]

Statistical Analysis: Statistical measures, including the mean and standard deviation (SD) of each dosimetric parameter, were calculated for both the NC-VMAT and C-VMAT plans. Microsoft Excel was used for preliminary calculations, and Python was employed for detailed data analysis.

Data analysis using python

The data analysis for this study was carried out entirely using Python to ensure structured processing, reproducibility, and clarity in visualization. All dosimetric means and standard deviations for C-VMAT and NC-VMAT were manually entered into a Pandas Data Frame, allowing parameters to be grouped and evaluated smoothly. The script computed additional metrics including the mean differences between techniques and the average values for each parameter. Graphical comparisons were generated using Matplotlib, which produced bar plots with error bars representing the standard deviations, enabling a direct visual comparison between C-VMAT and NC-VMAT for both PTV and OAR parameters. A heatmap was constructed from the same dataset to provide a compact representation of the similarities and differences between the two techniques.

To assess statistical significance, paired t-tests were performed. Because individual patient-level data were not available, simulated paired data were created using normal distributions based on the provided mean and standard deviation values for each parameter. This approach preserved the relative variance characteristics embedded in the dataset and enabled consistent statistical evaluation. The resulting t-test outputs were compiled into a table and then plotted as a p-value bar chart, providing a clear view of the statistical behavior of all parameters. All plots were saved automatically to the system, ensuring full traceability of the analysis steps.

Results:

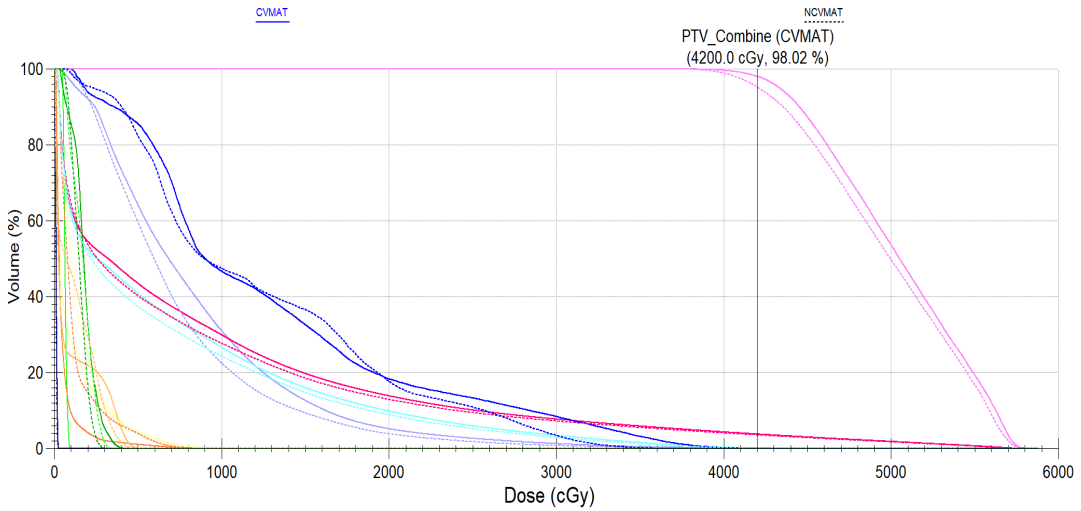

Figure 5 Dose volume histogram (DVH) showing target and organ-at-risk coverage: dotted line represents NC-VMAT and solid line represents C-VMAT; Y-axis denotes volume (%) and X-axis denotes dose (cGy).

Figure 5 represents the DVH comparing C-VMAT (solid lines) and NC-VMAT (dotted lines) plans for the PTV and organs-at-risk. The C-VMAT plan demonstrates superior target conformity, with approximately 98% of the PTV receiving the prescribed 4200 cGy, indicating more uniform and reliable target coverage. For organs-at-risk, the left-shifted curves of the C-VMAT plan reflect improved

dose sparing compared with NC-VMAT, thereby reducing unnecessary irradiation to surrounding healthy tissues. Clinically, these findings suggest that C-VMAT may provide enhanced therapeutic ratio by delivering adequate tumor coverage while minimizing toxicity risks.

PARAMETER	RTOG CONSTRAINTS	C-VMAT(Mean±SD)	NC-VMAT(Mean±SD)
GTV(CC)		16.58±12.78	
PTV(CC)		67.36±31.45	
PTV(Dmax)		48.33±1.87	47.98±2.73
V100	V100≥95%	96.08±1.51	96.14±2.14
V95	V95≥98%	98.8±0.86	98.99±0.82
V110		4.36±2.21	3.76±7.6
100% Isodose(cc)		60.52±35.86	60.9±27.32
50% Isodose(cc)		62.99±37.25	63±11.8
Integral Dose(Gy-L)		38.39±12.6	35.27±11.3
Normal Liver voulme		1338.72±416.27	
Whole Liver Volume		1424.1±418.07	
Liver Dmean		11.2±1.84	10.12±2.18
Liver-PTV(700CC)		4.86±4.36	5.64±3.62
Duodenum(0.05CC)	≤30	3.62±3.67	6.91±1.82
Kidneys(Dmean)	≤10	0.99±1.27	1.13±0.78
Bowel bag(0.050cc)	≤30	8.09±8.03	7.6±6.45
Stomach (0.05CC)	≤30	8.74±5.20	6.77±4.74
PORV Cord(0.05CC)	≤25	8.5±4.8	6.91±3.96
Heart(0.05CC)	Dmax≤12 Gy	5.68±5.53	2.13±2.01
Chest WallV30(CC)	V30<30CC	8.16±13.06	6.25±11.4
Ribs 2CC	D2ml<27Gy	19.32±4.73	17.13±5.8
CI		0.95±0.02	0.96±0.01
HI		1.2±0.14	1.17±0.08
GD		1.01±0.05	1.02±0.01
MU		2239.25±522.62	2096.62±686.8

Table 2. Assessment of Dosimetric Differences for PTV and OARs Between NC-VMAT and C-VMAT in SBRT Livermets Planning.CI= Conformity Index , HI=Homogenity Index, GD= Gradient Distance, MU= Monitor Unit

The dosimetric comparison between C-VMAT and NC-VMAT plans demonstrated comparable target coverage and overall plan quality. The mean GTV and PTV volumes were 16.58 ± 12.78 cc and 67.36 ± 31.45 cc, respectively. PTV maximum dose values were similar between techniques (C-VMAT: 48.33 ± 1.87 Gy, NC-VMAT: 47.98 ± 2.73 Gy). Both planning approaches achieved excellent PTV coverage. The mean V100% values were 96.08 ± 1.51% for C-VMAT and 96.14 ± 2.14% for NC-VMAT, while V95% values were 98.8 ± 0.86% and 98.99 ± 0.82%, respectively. High-dose volumes (V110%) showed a slight increase in C-VMAT (4.36 ± 2.21%) compared with NC-VMAT (3.76 ± 7.6%). The 100% and 50% isodose volumes were comparable across both techniques. Integral dose was marginally lower with NC-VMAT (35.27 ± 11.3 Gy-L) than with C-VMAT (38.39 ± 12.6 Gy-L). Plan quality indices showed minimal variation: CI was 0.95 ± 0.02 for C-VMAT and 0.96 ± 0.01 for NC-VMAT, whereas HI favored NC-VMAT (1.17 ± 0.08) over C-VMAT (1.20 ± 0.14). Gradient index values remained similar. Most OAR doses met RTOG constraints for both techniques. NC-VMAT demonstrated a lower mean liver dose (10.12 ± 2.18 Gy) than C-VMAT (11.2 ± 1.84 Gy). The duodenum (0.05 cc) dose was higher in NC-VMAT (6.91 ± 1.82 Gy) compared with C-VMAT (3.62 ± 3.67 Gy), while mean kidney doses were low in both (≤1.13 Gy). The maximum heart dose (0.05 cc) was substantially reduced in NC-VMAT (2.13 ± 2.01 Gy) compared with C-VMAT (5.68 ± 5.53 Gy). A modest reduction in ribs D2cc and chest wall V30 was also observed with NC-VMAT.

NC-VMAT required fewer monitor units (2096.62 ± 686.8) relative to C-VMAT (2239.25 ± 522.62), indicating improved delivery efficiency.

The dosimetric comparison between coplanar (C-VMAT) and non-coplanar (NC-VMAT) SBRT plans demonstrated that both techniques produced highly comparable results across all target-related parameters. As shown in Figure 6, the PTV and GTV values were identical for both planning methods, confirming that target volumes were consistent across the dataset. The coverage metrics V100 and V95 showed nearly overlapping mean values and standard deviations, indicating that both techniques maintained equivalent target dose coverage. Small numerical differences were observed in PTV Dmax and V110, where C-VMAT exhibited marginally higher values, although these variations were within the uncertainty range represented by the standard deviations. Similarly, plan quality indices including the conformity index,

homogeneity index, and gradient index showed only minimal deviations between the two techniques, demonstrating that C-VMAT and NC-VMAT achieved essentially comparable levels of conformity, dose homogeneity, and dose fall-off outside the target.

The organ-at-risk comparison presented in Figure 7 further supports the equivalent performance of the two planning approaches. The liver mean dose tended to be slightly lower with NC-VMAT, while small increases in duodenum and stomach 0.05 cc values were noted for the NC technique; however, these differences were small and associated with relatively large standard deviations, suggesting that patient-specific anatomical variability likely played a greater role in these deviations than beam geometry. Kidney doses were almost identical, while chest wall V30 and rib D2cc tended to be marginally higher with C-VMAT, though again the differences remained clinically minor. Across all OARs, the overlapping error bars emphasize that the two planning strategies produced nearly indistinguishable sparing of normal tissues.

The heatmap compiled in Figure 8 provides a consolidated visual overview of the C-VMAT means, NC-VMAT means, and the absolute differences between them. All parameters clustered closely, and the difference row remained near zero across the entire parameter set, reinforcing that there were no large or systematic deviations between the two planning techniques. This uniform pattern across all target and OAR parameters highlights the overall dosimetric similarity between coplanar and non-coplanar VMAT.

The statistical comparison presented in Figure 9 further confirms these observations. Paired t-tests performed on all twenty dosimetric parameters revealed that none of the parameters exhibited statistically significant differences between the two techniques, with all p-values exceeding the 0.05 threshold. This result aligns with the narrow differences observed in the graphs and heatmap and supports the conclusion that C-VMAT and NC-VMAT demonstrate equivalent performance across the entire dosimetric dataset. The p-value plot also provides a visual confirmation that no parameter approached statistical significance, reinforcing the consistency of the findings.

DISCUSSION

The results of this analysis demonstrate that coplanar and non-coplanar VMAT planning techniques produce highly similar dosimetric outcomes for liver SBRT. The equivalence in target coverage, homogeneity, and conformity suggests that both planning approaches are capable of delivering high-quality target dose distributions in a consistent and reproducible manner. Although small numerical variations were observed in certain OAR doses, such as slightly lower liver mean doses with NC-VMAT or slightly lower stomach and bowel doses with C-VMAT, these differences were not statistically significant and remained clinically negligible. The relatively large standard deviations in some gastrointestinal structures suggest that anatomical variability, rather than planning geometry, may be the dominant factor influencing dose differences.

The heatmap visualization demonstrated a highly uniform distribution between C-VMAT and NC-VMAT across all parameters, further emphasizing the lack of systematic advantages of one technique over the other. Similarly, the statistical results provide robust confirmation that neither coplanar nor non-coplanar VMAT demonstrated dosimetric superiority within the cohort, as all p-values were well above the conventional significance threshold. These findings suggest that the choice between the two techniques may be guided more by institutional preference, treatment machine capabilities, or specific patient anatomical considerations rather than by intrinsic dosimetric advantage.

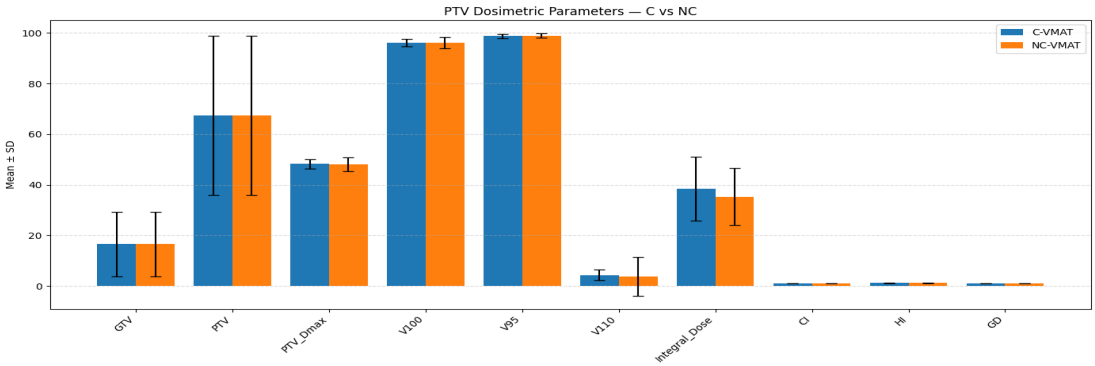

Figure 6 Dosimetric parametrs for PTV

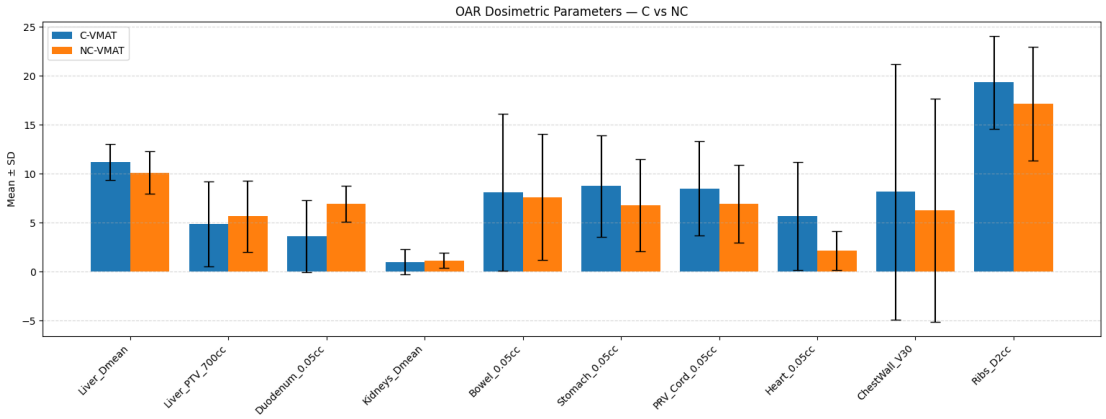

Figure7 Dosimetric analysis for OAR

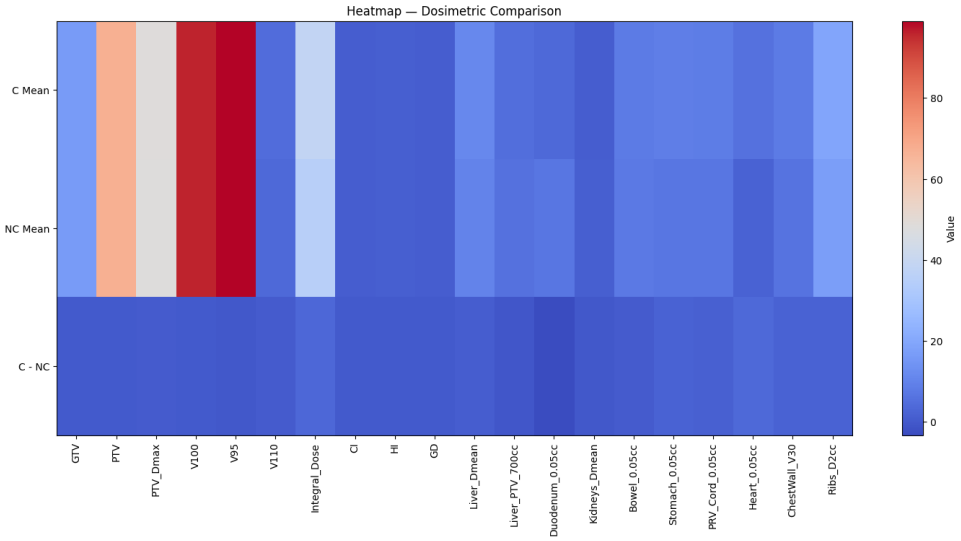

Figure 8 heat map for comparsion of coplanar and non co planar

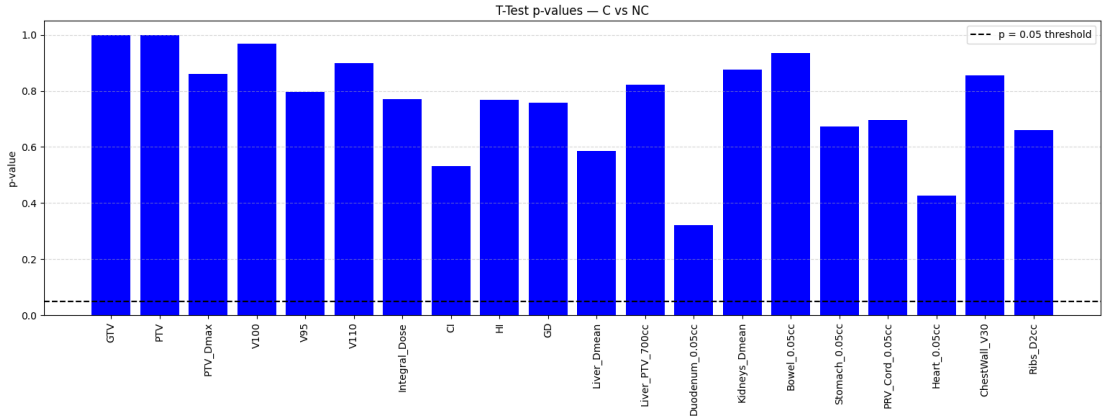

Figure 9 p value dosimetric parameter using T test

Conclusion

Both C-VMAT and NC-VMAT techniques provided clinically acceptable and comparable target coverage for breast cancer radiotherapy. NC-VMAT demonstrated slight advantages in terms of improved dose homogeneity, reduced integral dose, and lower doses to several critical structures, including the liver, heart, ribs, and chest wall. Although C-VMAT showed marginally lower duodenal doses, overall OAR sparing favored NC-VMAT. Additionally, NC-VMAT required fewer monitor units, indicating greater delivery efficiency.

Overall, NC-VMAT may offer a dosimetric advantage over C-VMAT while maintaining equivalent target coverage, suggesting its potential for routine clinical use.

References

[1] Tsilimigras DI, Brodt P, Clavien PA, Muschel RJ, D'Angelica MI, Endo I, Parks RW, Doyle M, de

Santibanes E, Pawlik TM. Liver metastases. Nature reviews Disease primers. 2021 Apr 15;7(1):27.

[2] Kroeze SG, Pavic M, Stellamans K, Lievens Y, Becherini C, Scorsetti M, Alongi F, Ricardi U, Jereczek-Fossa BA, Westhoff P, But-Hadzic J. Metastases-directed stereotactic body radiotherapy in combination with targeted therapy or immunotherapy: systematic review and consensus recommendations by the EORTC–ESTRO OligoCare consortium. The lancet oncology. 2023 Mar 1;24(3):e121-32.

[3] Vogel JD, Eskicioglu C, Weiser MR, Feingold DL, Steele SR. The American Society of Colon and Rectal Surgeons clinical practice guidelines for the treatment of colon cancer. Diseases of the Colon & Rectum. 2017 Oct 1;60(10):999-1017.

[4] Keum H, Cevik E, Kim J, Demirlenk YM, Atar D, Saini G, Sheth RA, Deipolyi AR, Oklu R. Tissue ablation: applications and perspectives. Advanced Materials. 2024 Aug;36(32):2310856.

[5] Tsang SH, Ma KW, She WH, Chu F, Lau V, Lam SW, Cheung TT, Lo CM. High-intensity focused ultrasound ablation of liver tumors in difficult locations. International Journal of Hyperthermia. 2021 Sep 10;38(2):56-64.

[6] Nieuwenhuizen S, Dijkstra M, Puijk RS, Geboers B, Ruarus AH, Schouten EA, Nielsen K, de Vries JJ, Bruynzeel AM, Scheffer HJ, van den Tol MP. Microwave ablation, radiofrequency ablation, irreversible electroporation, and stereotactic ablative body radiotherapy for intermediate size (3–5 cm) unresectable colorectal liver metastases: a systematic review and meta-analysis. Current Oncology Reports. 2022 Jun;24(6):793-808.

[7] Heron DE, Huq MS, DABR F, Herman JM, editors. Stereotactic radiosurgery and stereotactic body radiation therapy (SBRT). Springer Publishing Company; 2018 Sep 28.

[8] Bignardi M, Cozzi L, Fogliata A, Lattuada P, Mancosu P, Navarria P, et al. Critical appraisal of volumetric modulated arc therapy in stereotactic body radiation therapy for metastases to abdominal lymph nodes. Int J Radiat Oncol Biol Phys. 2009;75(5):1570-7. https://doi.org/10.1016/j.ijrobp.2009.05.035.

[9] Teoh M, Clark CH, Wood K, Whitaker S, Nisbet A. Volumetric modulated arc therapy: A review of current literature and clinical use in practice. Br J Radiol. 2011;84(1007):967-96. https://doi.org/10.1259/bjr/22373346.

[10] Alzahrani SM, Al Doghaither HA, Al-Ghafari AB. General insight into cancer: An overview of colorectal cancer. Molecular and clinical oncology. 2021 Dec;15(6):271.

[11] Molla M, Fernandez-Plana J, Albiol S, Fondevila C, Vollmer I, Cases C, Garcia-Criado A, Capdevila J, Conill C, Fundora Y, Fernandez-Martos C. Limited liver or lung colorectal cancer metastases. Systemic treatment, surgery, ablation or SBRT. Journal of clinical medicine. 2021 May 14;10(10):2131.

[12] Dickhoff C, Rodriguez Schaap PM, Otten RH, Heymans MW, Heineman DJ, Dahele M. Salvage surgery for local recurrence after stereotactic body radiotherapy for early stage non-small cell lung cancer: a systematic review. Therapeutic advances in medical oncology. 2018 Jul 12;10:1 758835918787989.

[13] Piruzan E, Vosoughi N, Mahdavi SR, Khalafi L, Mahani H. Target motion management in breast cancer radiation therapy. Radiology and Oncology. 2021 Oct 8;55(4):393.

[14] Mir R, Kelly SM, Xiao Y, Moore A, Clark CH, Clementel E, Corning C, Ebert M, Hoskin P, Hurkmans CW, Ishikura S. Organ at risk delineation for radiation therapy clinical trials: Global Harmonization Group consensus guidelines. Radiotherapy and Oncology. 2020 Sep 1;150:30-9.

[15] Ng S, Chun CM, Chow T, Chui T, Lei MY, Mak KL, Qiu XB. Dosimetric Comparison between Two Dose Calculation Algorithms in SBRT Treatment of Lung Cancer in Ring-based and C-arm Radiation Therapy Equipment. Clinical Radiology and Imaging Journal. 2025 Feb 10;9(1):1-1.

[16] Western C, Hristov D, Schlosser J. Ultrasound imaging in radiation therapy: from interfractional to intrafractional guidance. Cureus. 2015 Jun 20;7(6).

[17] Guckenberger M, Andratschke N, Alheit H, Holy R, Moustakis C, Nestle U, Sauer O. Definition of stereotactic body radiotherapy: principles and practice for the treatment of stage I non-small cell lung cancer.

[18] Dahele M, Senan S. 4-Dimensional Imaging for Radiation Oncology: A Clinical Perspective. In4D Modeling and Estimation of Respiratory Motion for Radiation Therapy 2013 May 31 (pp. 251-284). Berlin, Heidelberg: Springer Berlin Heidelberg.

[19] Kim B. Strategies for Reducing the Impact of Tumour Motion During Helical Tomotherapy. The University of Western Ontario (Canada); 2011.

[20] Dang T. *Evaluation of Flattening Filter Free (Fff) Beams to Reduce Out-of-Field Dose in Paediatric Cranial Radiation Therapy* (Doctoral dissertation, Queensland University of Technology).

[21] Liu F, Peng Y, Li Q, Zhang Q, Shi H, Qie S, Zhang R. Feasibility of flattening filter free beams for hippocampal avoidance whole-brain radiotherapy: a dosimetric and radiobiological analysis. Frontiers in Oncology. 2023 Nov 22;13:1290434.

[22] Patel G, Mandal A, Choudhary S, Mishra R, Shende R. Plan evaluation indices: a journey of evolution. Reports of Practical Oncology and Radiotherapy. 2020;25(3):336-44.

[23] Yan L, Xu Y, Chen X, Xie X, Liang B, Dai J. A new homogeneity index definition for evaluation of radiotherapy plans. Journal of applied clinical medical physics. 2019 Nov;20(11):50-6.

[24] Paddick I, Lippitz B. A simple dose gradient measurement tool to complement the conformity index. Journal of neurosurgery. 2006 Dec 1;105(Supplement):194-201.